

doi: 10.3788/gzxb20174607.0706003

基于回音壁模式微球腔的 PDH 稳频技术

王梦宇, 金雪莹, 王静, 陈黎明, 王克逸

(中国科学技术大学 精密机械与精密仪器系, 合肥 230026)

摘 要: 光学微球腔因其回音壁模式可获得极高的品质因数而受到广泛关注. 本文分析了 Fabry-Perot 腔和微球腔的基本原理, 通过 CO₂ 激光熔融光纤实验制得了直径为 1.2 mm 的微球腔, 并测试了微球腔和锥形光纤耦合结构的耦合特性. 采用典型的 PDH 稳频系统设计了基于微球腔的稳频系统, 分析了用于鉴频的误差曲线的吸收特性和色散特性, 对比了不同调制频率、微球腔直径、耦合损耗、传输损耗下与误差曲线斜率的关系. 结果表明: 耦合状态下最大 Q 值可达到 1.1×10^8 , 调节微球腔内横磁模和横电模的转换可优化耦合效率, 匹配微球腔和锥形光纤的尺寸得到了径向二阶模式的透射谱, 误差曲线效率达到 15.4 A mW/MHz. 球腔在提高 PDH 稳频技术灵敏度上具有巨大潜力.

关键词: 光纤光学; 激光稳频; 光学微球腔; PDH; 回音壁模式

中图分类号: TN815; TN24

文献标识码: A

文章编号: 1004-4213(2017)07-0706003-8

Analysis of the Pound-Drever-Hall Frequency Stabilization Technique Based on a Whispering Gallery Mode Optical Microsphere Cavity

WANG Meng-yu, JIN Xue-ying, WANG Jing, CHEN Li-ming, WANG Ke-yi

(Department of Precision Machinery and Precision Instrumentation, University of Science and Technology of China, Hefei 230026, China)

Abstract: Optical microsphere (OM) cavities supporting Whispering Gallery Modes (WGMs) have received much attention because of their high quality factor (Q). The study analyzes the Fabry-Perot (FP) cavity and OM cavity theories. An OM cavity with diameter of 1.2 mm was produced by melting a silica optical fiber using a CO₂ laser, and the coupling structure for OM cavity and tapered fiber was tested. We designed an OM cavity frequency stabilization system based on basic PDH frequency stabilization system. Absorption and dispersion characteristics of error signal curves used to be frequency discrimination curves were analyzed. We compared the relationships between error signal slopes and different modulation frequency, OM cavity's diameter, coupling loss, transmission loss. The results show that the maximum Q factor of OM cavity coupled by the tapered fiber is 1.1×10^8 . Transverse electric (TE) mode and transverse magnetic (TM) mode can be transformed to optimize coupling efficiency. The transmission spectrum of the second radial mode was obtained by matching dimensions between OM cavity and tapered fiber. The slope of the error signal is 15.4 A mW/MHz. Our work shows its potential to improve the sensitivity of the PDH technique.

Key words: Fiber optics; Laser frequency stabilization; Optical microsphere cavity; PDH; Whispering gallery mode

OCIS Codes: 060.2310; 140.4780; 120.2230; 120.4640; 060.2630

Foundation item: The National Natural Science Foundation of China (No. 61275011)

First author: WANG Meng-yu (1992-), male, M. S. degree candidate, mainly focuses on fiber optic and optical cavity. Email: mengyu@mail.ustc.edu.cn

Supervisor (Corresponding author): WANG Ke-yi (1962-), male, professor, Ph. D. degree, mainly focuses on micro-optic devices and digital optical information processing. Email: kywang@ustc.edu.cn

Received: Jan. 1, 2017; **Accepted:** Mar. 22, 2017

<http://www.photon.ac.cn>

0 Introduction

Optical Microsphere (OM) cavities^[1] have attracted considerable research^[2-3] over the last several years due to the high Q factor and small mode volume for a wide variety of applications, such as narrow linewidth micro-laser^[4-5], high-sensitivity sensors^[6-7], and narrow bandwidth optical filter^[8]. For the Whispering Gallery Modes (WGMs) of fused OM cavities, the Q factor can reach 10^9 or higher^[9].

Pound-Drever-Hall (PDH) frequency stabilization system was established by Drever and Hall in 80's last century, for inspiring of Pound's microwave frequency stabilization method^[10]. Generally, PDH frequency stabilization is an efficient technique for improving a prevailing laser^[11]. A general method makes use of FP cavity to get the standard frequency, which can lock laser frequency. A great advantage of PDH technique is that it is not limited by the waveband^[12]. However, high Q factor FP cavity is too expensive, and it needs a vacuum equipment which is costly and heavy, so it limits the application of FP cavity completely. To improve frequency stabilization in PDH technique, a modified method is proposed by using an OM cavity supporting WGMs. OM cavity has narrow Full Width At Half Maximum (FWHM), high Q factor, making it potential for frequency stabilization applications^[13]. The microsphere resonator is one of the key elements in PDH technique. In this letter, we present the locking of a laser into an OM cavity, featuring Q factor up to 10^8 .

1 Theoretical framework

The basic idea of PDH technique is to lock the laser frequency by providing optical reference cavity frequency. So it relies on a reference frequency provide by resonance cavity and then the sideband spectrum produced by phase modulation to achieve optical heterodyne detection. Therefore, Q factor of different cavities directly affects frequency stabilization effect and decides sensitivity and Linear Dynamic Range (LDR) of the frequency locking system.

1.1 FP cavity

FP cavity is a kind of traditional resonator cavity, mainly using two parallel plane mirrors to form a laser resonator, making it output laser directionally. The structure of FP cavity is shown in Fig. 1. The reflectivity of the two mirrors directly determines the Q factor of FP cavity and improving the foundry technics of the mirror coatings will increase reflectivity and Q factor. It is reported that the maximum Q factor can be improved to 10^5 but manufacture process will be too expensive.

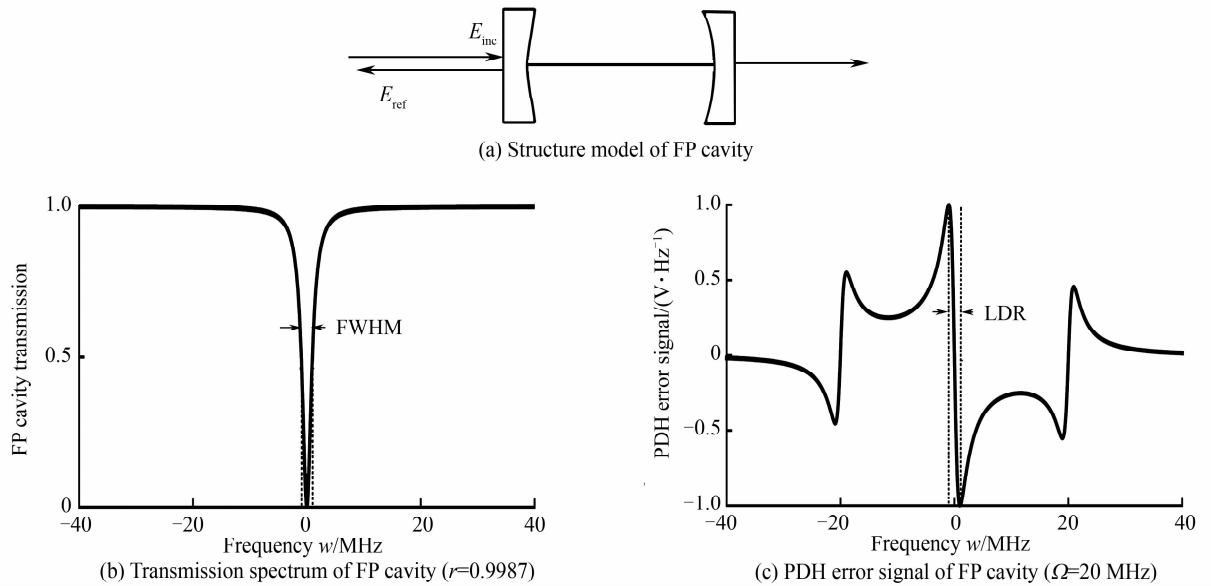


Fig. 1 The structure model, transmission spectrum curve and error signal curve of FP cavity

To describe the behavior of the reflected beam quantitatively, the electric field of incident beam can be written as: $E_{inc} = E_0 \exp(i\omega t)$, the electric field of the reflected beam is: $E_{ref} = E_1 \exp(i\omega t)$. we account for the relative phase between the two waves by letting E_0 and E_1 be complex. The reflection coefficient $F(\omega)$

is the ratio of E_{ref} and E_{inc} , it can be given by^[14]

$$F(\omega) = E_{\text{ref}}/E_{\text{inc}} = \frac{r \cdot [1 - \exp(i\omega/\text{FSR})]}{1 - r^2 \cdot \exp(i\omega/\text{FSR})} \quad (1)$$

where r is the amplitude reflection coefficient of each mirror, and $\text{FSR}=c/2L$ is the free spectral range of FP cavity of length L . The transmission spectrum of the FP cavity can be obtained by simulation and the PDH error signal curve can also be got by simulation after Frequency Modulation (FM), which are shown in Fig. 1. And the transmission spectrum and the PDH error signal curve of the FP cavity will be analyzed in the subsequent sections.

1.2 OM cavity

The WGMs of OM cavity make the optical waves in the interface of cavity generate inner total reflection constantly, then form a steady transmission state. This state constrains optical waves in the microcavity, endowed with minimal optical depletion. Hence, OM cavity has excellent advantages such as high Q factor and small mode volume.

OM cavity was produced by melting a silica optical fiber using a CO_2 laser^[15]. In the experiment, when optical fiber absorbed light energy, the fiber would melt and form an optical microsphere cavity. The radius of the cavity (R) can be controlled by changing the length between fiber and laser (L). They meet approximately: $R \approx (2930L)^{1/3} \mu\text{m}$ due to the same volume of the fiber^[16]. The method is appropriate for the production of OM cavity, whose diameter is more than $300 \mu\text{m}$. Hydrofluoric acid (HF) can be used to acquire lower mode volumes OM cavity, whose diameter is $10 \sim 300 \mu\text{m}$. Additionally, a tapered fiber, which is fabricated by using the method of heat-and-pull method, must be used to excite WGMs of intracavity. The coupling structure of OM cavity and tapered fiber is shown in Fig. 2.

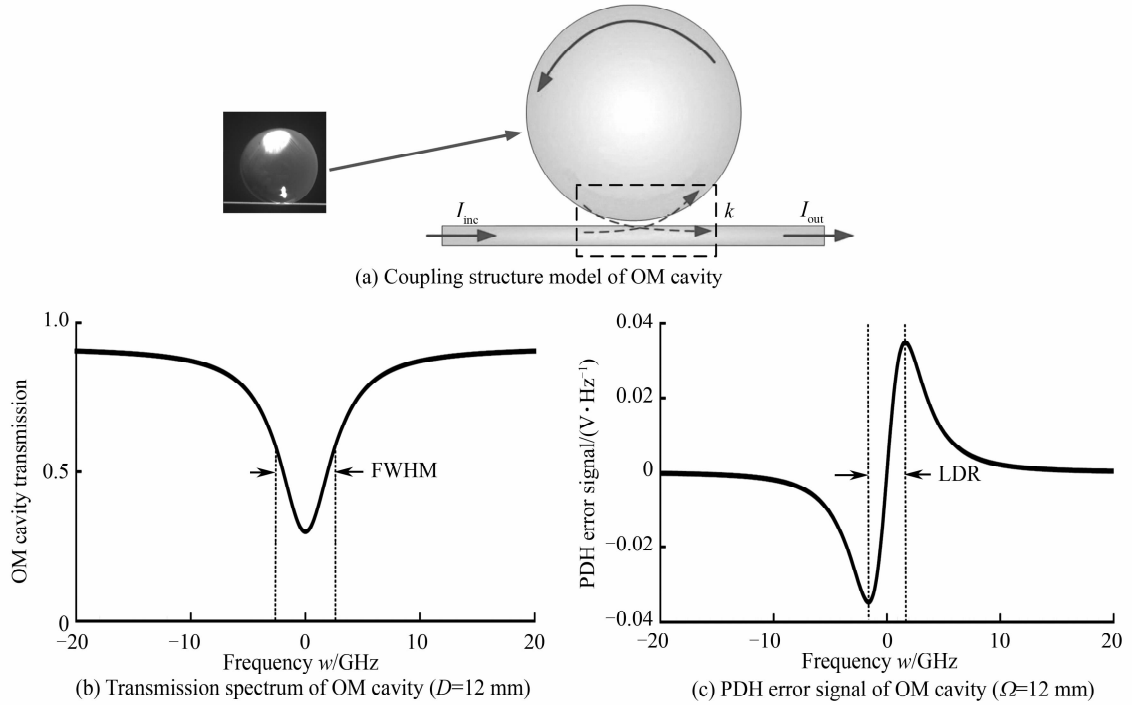


Fig. 2 The coupling structure model, transmission spectrum curve and error signal curve of OM cavity

To describe the behavior of the reflected beam quantitatively, the optical field of incident beam can also be written as: $I_{\text{inc}} = I_0 \exp(i\omega t)$. the optical field of the reflected beam is: $I_{\text{out}} = I_1 \exp(i\omega t)$. The reflection coefficient $T(\omega)$ is the ratio of I_{out} and I_{inc} , it is given by multiple-beam interference principle^[17]

$$T(\omega) = \frac{I_{\text{out}}}{I_{\text{inc}}} = A - B \cdot \frac{1 - C^n \cdot \exp(-i\omega n/\text{FSR})}{1 - C \cdot \exp(-i\omega/\text{FSR})} \exp(-i\omega/\text{FSR}) \quad (2)$$

where $A = (1-k)^{1/2} (1-L)^{1/2}$, $B = k(1-L)^{1/2} (1-e)^{1/2}$, $C = (1-k)^{1/2} (1-L)^{1/2} (1-e)^{1/2}$, and k , L , e are the coupling loss, deterioration loss, transmission loss of coupling structure, and $\text{FSR}=c/\pi nD$ is the free spectral range of OM cavity. Deterioration loss L is usually zero because of its high Q factor. The

simulation result of transmission spectrum and the PDH error signal curve of OM cavity are shown in Fig. 2 and will be analyzed in the subsequent sections.

2 Experimental results and discussion

2.1 Detection of resonant spectrum of OM cavity

A detection system of resonance spectrum of OM cavity can be established, which mainly consists of wave tunable laser, signal generator, polarization controller, photo detector and oscilloscope, as shown in Fig. 3. Specifically, wave tunable laser driven by triangular-wave signal produced by the signal generator conducts wavelength scanning. Isolator protects the laser from reflected light. Light from laser enters tapered fiber, and then couples into OM cavity. Photo detector can convert light signal to electrical signal displayed in the oscilloscope. When the laser wavelength scans the WGM of OM cavity, a large portion of the laser will couple into OM cavity, then presents obvious resonance peaks in the OM cavity transmission, which is shown as Fig. 3. Q factor can be obtained by measuring FWHM of resonance peaks and different Q factors can be obtained by adjusting the distance between OM cavity and tapered fiber.

To have a better understanding of the electric field of intra-cavity, four parameters can be used to describe it: p expresses the polarization state of OM cavity, q expresses the number of radial modes, l expresses the number of angular mode, m expresses the number of azimuthal modes. TE mode and TM mode can be transformed by adjusting polarization controller to realize arouse fundamental mode ($q=1$, $m=1$) of intra-cavity efficiently. According to Fig. 3, it can be noticed that different resonant mode presents various Q factors and various coupling efficiency. The maximum Q factor can reach to 1.1×10^8 , but the coupling efficiency relatively low. Fortunately, coupling efficiency of resonance peak 1 will become increasing when TE mode and TM mode are transformed, which can be considered as a method to optimize performance of resonance mode.

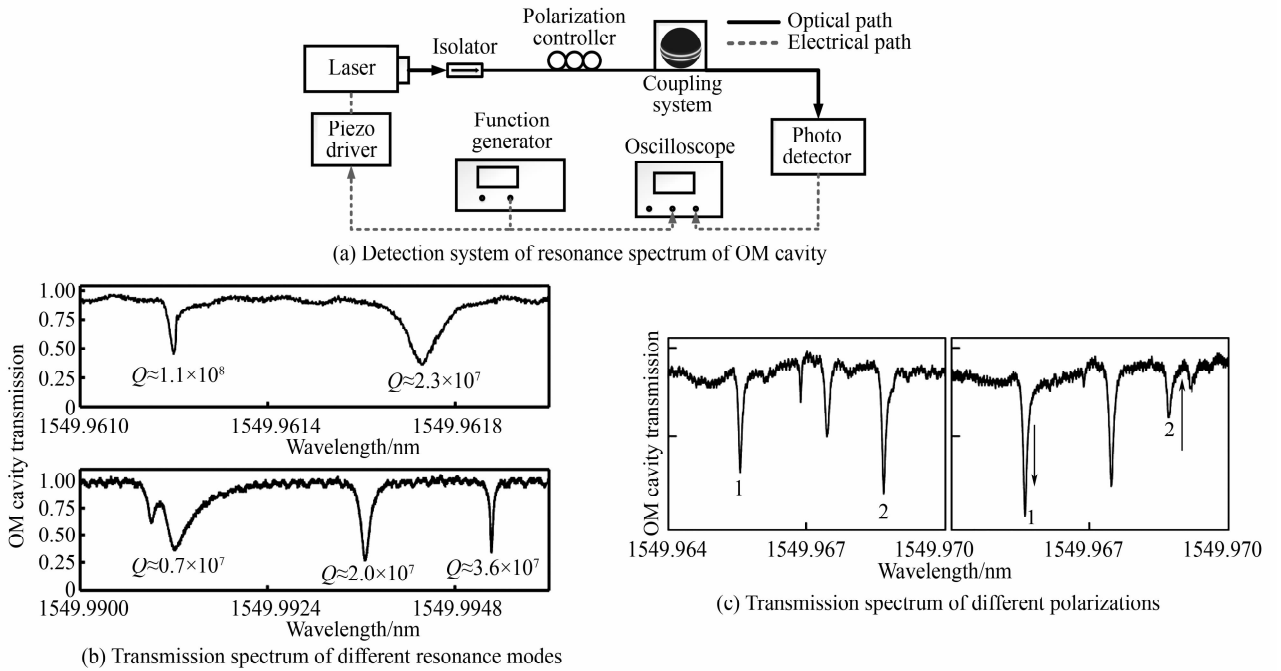


Fig. 3 The schematic diagram of detection system and transmission spectrum

2.2 Dimensions matching between coupling structure for OM cavity and tapered fiber

Coupling structure needs to match the dimensions to arouse fundamental mode. Waist diameter of tapered fiber by heat-and-pull method is changing gradually, means that coupling state will be affected when OM cavity moves along tapered fiber. The transmission spectrum of OM cavity coupling with a tapered fiber in different zones is shown in Fig. 4. It can be summarized that the left area transmission should belong to the first order model ($q=1$) and the right area transmission should belong to the second order model ($q=2$) according to Ref. [11]. Propagation constant of lower order radial mode will be bigger than that of higher order radial mode when WGM of angular mode is the same. Therefore,

resonance peaks of the second radial mode will get lower gradually, then resonance peaks of the first radial mode will get less when OM cavity moves along to broad waist of tapered fiber.

Additionally, temperature changes leads to the shift of the resonance wavelength. The relationship between WGM wavelength shift and temperature can be obtained as temperature rises. And temperature turning sensitivity of OM cavity measured by thermocouple is 13.85 pm/°C and the resolution of OM cavity temperature sensor is 1.12×10^{-4} °C. Parameters of OM cavity are listed in Table 1.

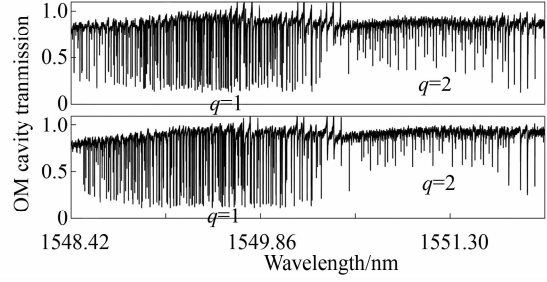


Fig. 4 Transmission spectrum of OM cavity coupling with tapered fiber in different zones

Table 1 Parameters of WGM OM cavity

Characteristics	Light wavelength	Index	diameter	The minimum coupling loss	The minimum FWHM	FSR	The maximum Q factor	Temperature turning sensitivity
Values	1550 nm	1.46	1.2 mm	2.7%	1.76 MHz	54.5 GHz	1.1×10^8	13.85 pm/°C

3 Theoretical results and simulation analysis

3.1 The PDH laser frequency stabilization system based on OM cavity

According to the basic PDH frequency stabilization system with FP cavity, the system of PDH technique is designed based on OM cavity. The setup is shown in Fig. 5.

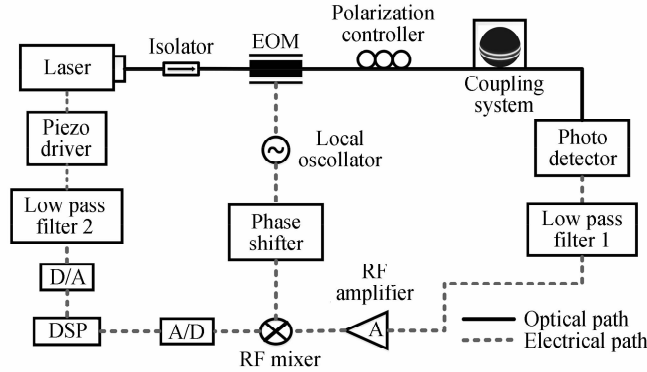


Fig. 5 The PDH laser frequency stabilization system based on OM cavity

A 1550 nm laser source goes through an Electro-optic phase modulator (EOM) and couples into tapered optical fiber. The output optical field of the coupling structure enters into the Photo Detector (PD) and is converted to electric field. Then the electric field passes in signal conditioning system. DSP is one of the core components of the signal conditioning system, mainly processes error signal. Finally, feedback signal enters into piezo driver (PZT-DR) of the laser. TE and TM mode can be transformed by adjusting Polarization Controller (PC). Isolator, which protects the laser from reflected light, and Phase Shifter (PS), which compensates phase delay caused by two unequal light paths, are indispensable in real applications. The modulated laser optical field is indicated as:

$$I_{in} = E_0 \cdot \exp(i\omega t + iB\sin \Omega t) \quad (3)$$

where ω , B , Ω are laser frequency, modulation depth and modulation frequency, respectively. Ignore higher order edge frequency components, so the output optical field of OM cavity can be written as

$$I_{out} \approx E_0 \cdot \{J_0(B)T(\omega)\exp(i\omega t) + J_1(B)T(\omega + \Omega)\exp[i(\omega + \Omega)t] - J_{-1}(B)T(\omega - \Omega)\exp[i(\omega - \Omega)t]\} \quad (4)$$

there are three strong frequencies after electric field modulation; 1) The laser intrinsic frequency ω ; 2) The sideband frequency $\omega + \Omega$ and $\omega - \Omega$ located in each part of ω ; Finally, the error signal after low pass filter 1,

RF mixer, DSP and low pass filter 2 can be obtained as

$$e = -2AP_0 J_0(B) J_1(B) \cdot \{ \text{Re}[T(\omega) T^*(\omega + \Omega) - T^*(\omega) T(\omega - \Omega)] \cos \Omega t + \text{Im}[T(\omega) T^*(\omega + \Omega) - T^*(\omega) T(\omega - \Omega)] \sin \Omega t \} \quad (5)$$

where $\cos \Omega t$, $\sin \Omega t$ expresses absorption and dispersion characteristics of the error signal. The error signal has superior features, such as central symmetry, big slope and large capture range. The bigger slope behaves, the greater effect frequency stabilization performs.

3.2 The characteristics of absorption line and dispersion line

From the analysis in the previous section, we can conclude that the curves of absorption line and dispersion line of the error signal can be obtained if real part and imaginary part were divided, which were shown in Fig. 6. A conclusion that the error signal presents absorption characteristic which FM is low, but converts to take on dispersion characteristic as FM is high, can be reached by simulation data.

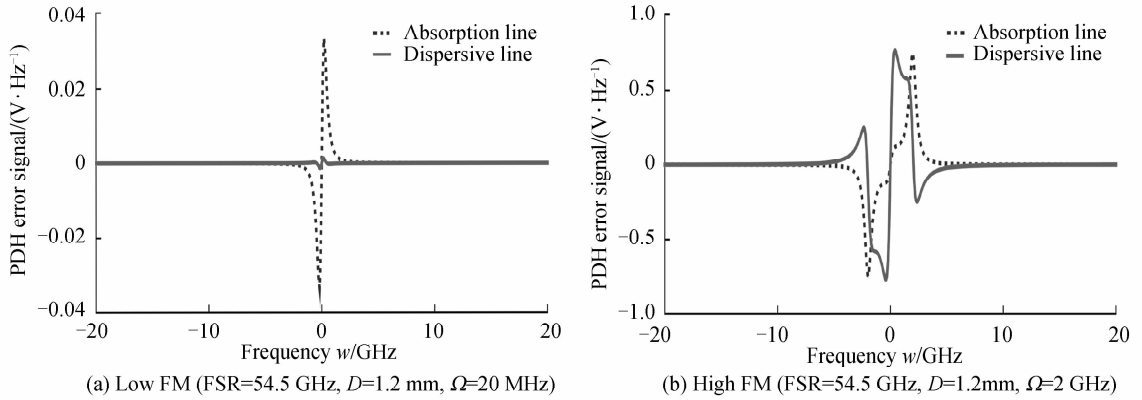


Fig. 6 The curves of absorption line and dispersion line

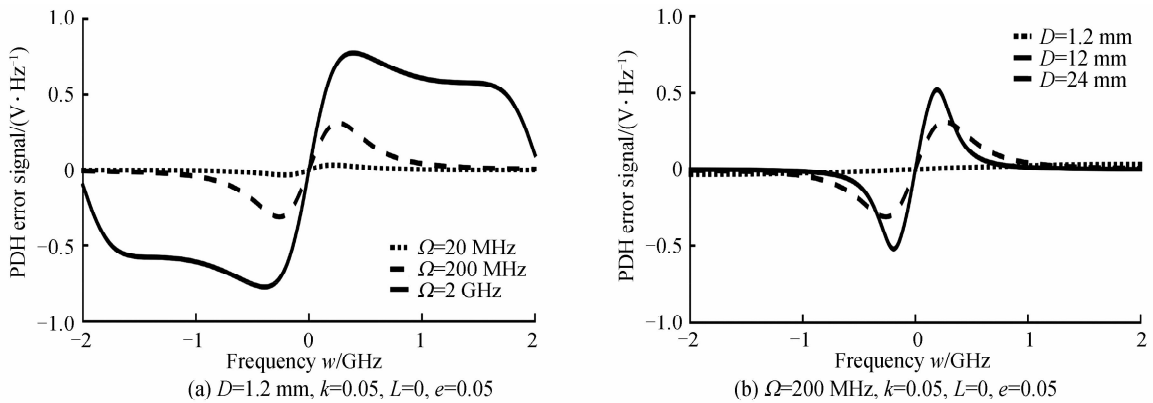
3.3 Relationship between slope of error signal and Ω , D , k , e

Dispersion line can be chosen to be frequency discrimination curve from Fig. 7, and when FM Ω becomes high ($\sin \Omega t = 1$), the error signal can be expressed as

$$e = -2AP_0 J_0(B) J_1(B) \cdot \text{Im}[T(\omega) T^*(\omega + \Omega) - T^*(\omega) T(\omega + \Omega)] \quad (6)$$

where A is amplitude gain of all demodulator circuits, P_0 is laser power, $J_0(B)$, $J_1(B)$ are Bessel functions.

Simulation data can express the relationships between the slopes of error signal and Ω , D , k , e as shown in Fig. 7. It can be noticed that the slope is bigger under high FM ($\Omega = 2$ GHz), means greater frequency stabilization effect. The best effect can be obtained when $\Omega = 2$ GHz, $D = 24$ mm, $k = 0.05$, $L = 0$, $e = 0.01$. Theoretical result should combine with process in practice to realize higher performance.



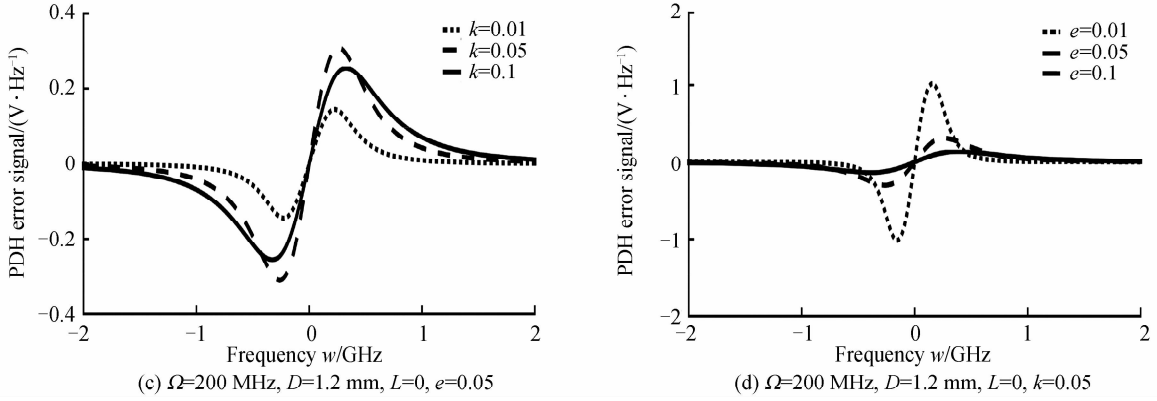


Fig. 7 The PDH error signal with different Ω , D , k , e

3.4 Comparison of frequency stabilization between OM cavity and FP cavity

When FM Ω is as big as 2 GHz, the slope can be obtained at the resonant point as

$$S = \left. \frac{d}{d\omega} e \right|_{\omega=\omega_{\text{res}}} = -2AP_0 J_0(B) J_1(B) \cdot \left. \frac{d}{d\omega} \text{Im}[T(\omega) T^*(\omega + \Omega) - T^*(\omega) T(\omega - \Omega)] \right|_{\omega=\omega_{\text{res}}} \approx -2AP_0 J_0(B) J_1(B) \cdot 2i \text{Im} T(\omega) \approx 8AP_0 J_0(B) J_1(B) / \text{FWHM} \quad (7)$$

where FWHM is inversely proportional to the Q factor. In order to get the largest slope of system, we choose $B=1.082$, $J_0(B) J_1(B)$ is as big as $0.339^{[18]}$. When laser power is 10mW, the slope can be calculated is

$$S \Big|_{\text{FWHM}=1.76 \text{ MHz}, B=1.082} = 15.4A \text{ mW/MHz} \quad (8)$$

According to Eq. (7), we notice that the stability of PDH technique can be affected two factors: amplitude gain A of demodulator circuits and FWHM of resonance cavity. The critical key of PDH technique is the resonance cavity with a narrow FWHM^[19]. The comparison of our frequency stabilization parameters with other experimental results is shown in Table 2. The slope can be optimized to realize high-performance sensors.

Table 2 Comparison of the PDH frequency stabilization effect

Number	Resonant cavity	FSR/MHz	FWHM/MHz	Slope/(mW·MHz ⁻¹)	Ref.
1. Delft, Netherland	FP cavity	375	2.9	0.67A	[20]
2. Heifei, China	OM cavity	5 450	1.76	15.4A	

From Table 2, the narrower FWHM of OM cavity corresponds to the bigger slope of the error signal, the same to the higher sensitivity of the PDH frequency stabilization system. Theoretically, FWHM of OM cavity can be reduced to 1 kHz. From the FWHM calculation equations, as is shown as Eq. (9), the parameters which impact FWHM are mainly fineness (F), diameter D and refractive index n .

$$\frac{d(\text{FWHM})}{dt} = \frac{1}{F} \frac{d(\text{FSR})}{dt} = \frac{1}{F} \frac{d(c/\pi n D)}{dt} = -\frac{1}{F} \frac{c}{\pi (nD)^2} \left(n \frac{dD}{dt} + D \frac{dn}{dt} \right) \quad (9)$$

We can conclude that the slope is determined by the parameters FM Ω , amplitude gain A , laser power P_0 , Bessel function $J_0(B) J_1(B)$ and FWHM of OM cavity from previous analysis. The sensitivity can be promoted by enlarging these parameters. FWHM depends on Q factor. Diameter D , refractive index n , coupling loss k and transmission loss L , can impact FWHM or Q factor. Moreover, adding coupling way, matching the dimensions of tapered fiber, transforming TE and TM mode can be considered to optimize coupling efficiency. The influence of indoor temperature on the refractive index n and transmission loss L should be avoided.

4 Conclusion

In conclusion, OM cavity was produced by melting a silica optical fiber using a CO₂ laser and parameters of OM cavity was obtained by testing the coupling structure for OM cavity and tapered fiber. The maximum Q factor is 1.1×10^8 , the FWHM is 1.76MHz, the resolution of temperature sensor is

1.12×10^{-4} °C. A novel PDH frequency stabilization system based on OM cavity is proposed instead of FP cavity. Dispersion line can be chosen to be frequency discrimination curve by simulation. Modulation frequency, diameter of OM cavity, coupling loss, transmission loss can have great impact on sensitivity of the error signal. The slope of error signal is 15.4A mW/MHz, so the modified method will improve sensitivity of PDH technique. Our work demonstrated here provides potential for PDH frequency stabilization applications.

References

- [1] VAHALA K J. Optical microcavities[J]. *Nature*, 2003, **424**(6950): 839.
- [2] ILCHENKOV S, MATSKO A B. Optical resonators with whispering-gallery modes-part II: applications[J]. *IEEE Journal of Selected Topics in Quantum Electronics*, 2006, **12**(1): 15-32.
- [3] MATSKO A B, ILCHENKO V S. Optical resonators with whispering-gallery modes-part I: basics[J]. *IEEE Journal of Selected Topics in Quantum Electronics*, 2006, **12**(1): 3-14.
- [4] ELLIOTT G R, MURUGAN G S, WILKINSON J S, *et al.* Chalcogenide glass microsphere laser[J]. *Optics Express*, 2010, **18**(25): 26720-26727.
- [5] MURUGAN G S, ZERVAS M N, PANITCHOB Y, *et al.* Integrated Nd-doped borosilicate glass microsphere laser[J]. *Optics Letters*, 2011, **36**(1): 73-75.
- [6] DONG C H, HE L, XIAO Y F, *et al.* Fabrication of high-Q polydimethylsiloxane optical microspheres for thermal sensing[J]. *Applied Physics Letters*, 2009, **94**(23): 839.
- [7] WANG H, YUAN L, KIM C W, *et al.* Optical microresonator based on hollow sphere with porous wall for chemical sensing[J]. *Optics Letters*, 2012, **37**(1): 94-96.
- [8] Wang P, DING M, MURUGAN G S, *et al.* Packaged, high-Q, microsphere-resonator-based add-drop filter[J]. *Optics Letters*, 2014, **39**(17): 5208-5211.
- [9] CHIASERAA, DUMEIGE Y, FERON P, *et al.* Spherical whispering-gallery-mode microresonators [J]. *Laser & Photonics Reviews*, 2010, **4**(3): 457-482.
- [10] DREVER W P, HALL J L, KOWALSKI F V, *et al.* Laser phase and frequency stabilization using an optical resonator[J]. *Applied Physics B*, 1983, **31**(2): 97-105.
- [11] CYGANA, LISAK D, WOJTEWICZ S, *et al.* Active control of the Pound-Drever-Hall error signal offset in high-repetition-rate cavity ring-down spectroscopy[J]. *Measurement Science & Technology*, 2011, **22**(11): 115303.
- [12] BRITAGERM, FRIEDRICH D, KROKER S, *et al.* Pound-Drever-Hall error signals for the length control of three-port grating coupled cavities[J]. *Applied Optics*, 2011, **50**(22): 4340-4346.
- [13] LIU Q, TOKUNAGA T, HE Z. Ultra-high-resolution large-dynamic-range optical fiber static strain sensor using Pound-Drever-Hall technique[J]. *Optics Letters*, 2011, **36**(20): 4044-4046.
- [14] BLACK D. An introduction to Pound-Drever-Hall laser frequency stabilization[J]. *American Journal of Physics*, 2001, **69**(1): 79-87.
- [15] DOMINGUEZ-JUAREZ L, KOZYREFF G, MARTORELL J. Whispering gallery microresonators for second harmonic light generation from a low number of small molecules[J]. *Nature Communications*, 2011, **2**(1): 254.
- [16] DONG Y, WANG K, JIN X. Package of a dual-tapered-fiber coupled microsphere resonator with high Q factor[J]. *Optics Communications*, 2015, **350**: 230-234.
- [17] BAUMGARTEL L M, THOMPSON R J, YU N. Frequency stability of a dual-mode whispering gallery mode optical reference cavity[J]. *Optics Express*, 2012, **20**(20): 29798-29806.
- [18] HU Shu-ling, GENG Wei-biao, YUAN Dan-dan, *et al.* PDH frequency stabilization signal detection technology[J]. *Infrared & Laser Engineering*, 2013, **42**(1): 233-238.
- [19] GUO Yong, QIU Qi, WANG Yun-xiang, *et al.* Research on stability of Fabry-Perot cavity based on PDH[J]. *Chinese Journal of Lasers*, 2016, **43**(4): 0402003.
- [20] SWINKELSB L. High accuracy absolute distance metrology[J]. *Applied Sciences*, 2006; 21.